applied optics

302 nm continuous wave generation by intracavity frequency doubling of a diode-pumped Pr:YLF laser

Na Niu,[1,*] Shuangshuang Pu,[1] Qing Chen,[1] Yan Wang,[1] Yue Zhao,[1] Wenjian Wu,[1] and Quan Zheng[1,2]

[1]Changchun New Industries Optoelectronics Technology Co., Ltd., Changchun 130012, China
[2]Changchun Institute of Optics, Fine Mechanics and Physics, The Chinese Academy of Science, Changchun 130033, China
*Corresponding author: niuna@cnilaser.com

Received 30 August 2018; revised 23 October 2018; accepted 24 October 2018; posted 25 October 2018 (Doc. ID 344641); published 16 November 2018

In this paper, we report on the intracavity frequency doubling of the Pr:YLF laser with a LiB_3O_5 (LBO) crystal, which was pumped by a combined 1.4 W blue laser diode at 444 nm and 1.5 W blue laser diode at 469 nm. By optimizing the design of the resonator, using a 5-mm-long LBO crystal, the maximum output power of 5 mW at 302 nm was achieved with respect to the total pump power.

https://doi.org/10.1364/AO.57.009798

1. INTRODUCTION

In recent years, as Pr^{3+}-doped materials could offer rich laser transitions in the visible spectral range, a considerable interest has emerged in the development of Pr^{3+}-doped crystal lasers. What is more, visible lasers could indeed open the access to ultraviolet (UV) or even deep-UV generation by one frequency doubling instead of two [1]. However, the use of Pr^{3+}-doped crystal lasers was somewhat limited by the lack of efficient pump sources in the blue region. Few years ago, a Pr^{3+}-doped crystal was pumped by a pulsed dye laser at 444 nm, flash-lamp, or Argon ion laser. During the last decade, with the development of pump sources such as optically pumped and frequency-doubled semiconductor lasers (OPSLs) and an InGaN laser diode, a series of very encouraging results was obtained with these pump sources. The frequency-doubled OPSL has always been used in high-power lasers, which was rather expensive. An InGaN laser diode at 444 nm was commonly used in low-power lasers, which has commercial availability and an acceptable price. Pr:YLF was considered the most promising material of all Pr^{3+}-doped fluorides [2], and many Pr:YLF-based visible wavelengths have been reported, such as 522 nm, 604 nm, 607 nm, 640 nm, 697 nm, and 720 nm [3–7], with the power of these visible lasers being even up to the watt level. The Pr:YLF-based ultraviolet wavelengths were reported as less than visible wavelengths, at only 261 nm, 303 nm, 320 nm, 349 nm, and 360 nm [8–13]. In this paper, to the best of our knowledge, we report on a Pr:YLF-based ultraviolet laser at 302 nm for the first time, as this wavelength could be used for a particular application.

In electric power systems, sulfur hexafluoride (SF_6) has been widely used as an insulating medium. Due to the presence of electric arcs, sparks, or coronas, SF_6 can be decomposed into sulfur fluorides, which in turn react with electrodes and gas impurities to form various chemically active by-products (such as SOF_4, SOF_2, SO_2F_2, SO_2, CO, and H_2S). The monitoring of decomposed by-products is able to identify and determine the occurrence of faulty types in the electrical equipment and thus minimize security risks [14]. Therefore, it is critical to develop a sensitive, selective, and cost-effective SO_2 sensor in a SF_6 buffer gas environment for high-voltage electric power systems. The detection method of SO_2 has been mainly based on the laser absorption spectroscopy technique, which is fast, has high sensitivity, and is becoming the development direction of trace detection. To avoid cross-talk and obtain a high-detection sensitivity, the optimal wavelength region for the SO_2 detection in the SF_6 buffer gas was identified to range between 250 and 320 nm. In 2017, Yin *et al.* [15] report a highly sensitive SO_2 photoacoustic sensor for the application of SF_6 decomposition detection, using a diode-pumped solid-state laser emitting at 303.6 nm. It can be seen in Fig. 1. The absorption of SO_2 at the wavelength of 302 nm is much greater than that of 303.6 nm. Furthermore, other UV sources, such as the tunable deep-UV laser system, have the disadvantages of high price and large volume. Therefore, the study of a compact all-solid-state 302 nm ultraviolet laser to fulfill these spectral properties is of great significance.

2. EXPERIMENTAL SETUP

In this work, we obtained the 302 nm ultraviolet light by intracavity frequency doubling of the 604 nm transition in Pr:YLF

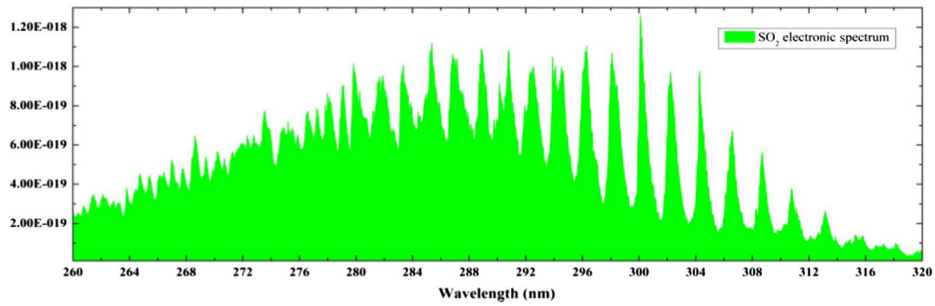

Fig. 1. Electronic absorption cross section of SO_2.

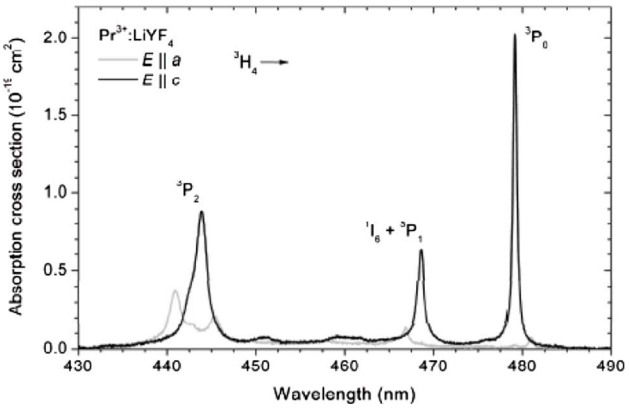

Fig. 2. Polarized absorption spectra of Pr:YLF in the blue spectral region.

($^3P_0 \rightarrow {}^3H_6$). There are three large absorption spectra in the blue band for the Pr:YLF crystal, which are 444 nm, 469 nm, and 479 nm, respectively, as shown in Fig. 2 [16]. With the maturity and commercialization of the blue led diode (LD), an increasing number of individuals choose a blue light diode as a pump source. However, the power has not been raised for one diode yet. The fiber coupling of two or several diodes will affect the polarization characteristics, resulting in a decreased absorption efficiency. The technique of combining light with two different wavelengths is more practical. On the one hand, the whole pump power can be increased, and on the other hand, the polarization characteristics of the pump light can be preserved, and the absorption efficiency can be improved.

The schematic experimental setup is depicted in Fig. 3. The pump source are two blue LDs from OSRAM Opto.

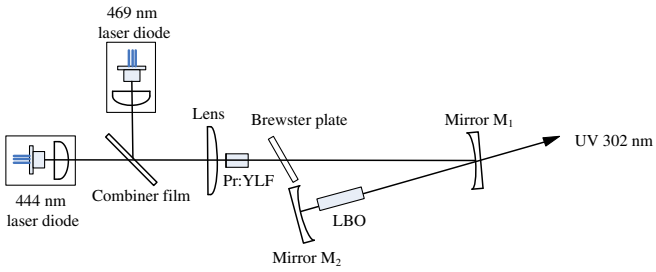

Fig. 3. Schematic setup of the blue-laser-diode-pumped Pr:YLF laser.

Semiconductors. One of them is emitting a linearly polarized light at $\lambda = 444$ nm, with a maximum output power of 1.4 W and a linewidth of 1.7 nm measured at the maximum output power. Another one is emitting a linearly polarized light at $\lambda = 469$ nm with a maximum output power of 1.5 W and a linewidth of 1.6 nm measured at the maximum output power. The M^2 parameters for LD at 444 nm (469 nm) are $M_x^2 = 17.8$ (10.7) and $M_y^2 = 2.1$ (1.8) in the x and y directions. The spectroscopic properties of Pr:YLF crystals regarding the polarized absorption and emission are well known [17,18]. To achieve a large absorption coefficient, the polarization absorption characteristic of Pr:YLF is taken into account, and therefore, the linearly polarized light of LDs was oriented so as to $E \| c$. In addition, the LDs were mounted on a cooper heat sink, and the temperature was controlled by thermoelectric cooler (TEC), which makes the wavelength of LDs overlap the absorption peak of the Pr:YLF crystal. The two LDs are collimated separately by a 4.2-mm-focal-length lens. Then, the two beams of LDs are combined with a combiner film, which is coated by our laboratory. The film was coated with AR at 444 nm and HR at 469 nm when the incidence is 45°. A 12-mm-focal-length lens was used to focus the pump beams into the laser crystal, resulting in a spot size of 84 × 90 μm (60 × 92 μm) for 444 nm (469 nm) LD, approximately.

As shown in Fig. 4, for the emission spectra of Pr:YLF, there was a wavelength at approximately 604 nm for the orange laser operation. Although the stimulated emission cross section at

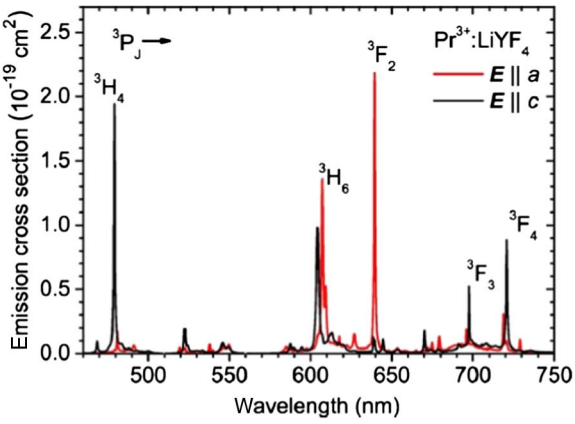

Fig. 4. Polarized emission spectra and effective emission cross section of Pr:YLF in the visible and deep-red spectral region.

604 nm is relatively large, the threshold value is increased due to the reabsorption loss of Pr:YLF, which affects the high-power output and really few reports on Pr:YLF-based wavelengths at 604 nm. The lower concentration of the crystal was considered as helpful in decreasing the probability of non-radiative cross-relaxation processes [19]. Considering this, a 8-mm-long Pr:YLF crystal with a low dopand concentration of 0.2 at. % Pr^{3+} in the crystal was used in our experiments. One side of the Pr:YLF crystal was antireflective (AR) coated for the pump wavelength at 444–469 nm and highly reflective (HR) coated for the fundamental wavelength at 604 nm as an input coupler; the other side of the Pr:YLF crystal was AR coated for 444–469 nm and 604 nm. For an intracavity frequency doubling of 604 nm, a 5-mm-long LiB_3O_5(LBO) crystal was used. The nonlinear crystal was designed for type I phase matching ($\theta = 90°$, $\varphi = 61.7°$). IIt is known that the UV AR coating has a very limited lifetime, which can be easily damaged, so the LBO crystal was cut with uncoated facets. The Pr:YLF and LBO were mounted on a copper heat sink, and the temperature was controlled by a thermal electric cooler.

A typical V-resonator can provide optimal beam waists, both in the nonlinear and gain crystal. The coated Pr:YLF crystal, M1, and M2 form the V-resonator. The mirror M1 was HR coated for 604 nm and AR coated for 302 nm with a radius of curvature of 100 mm, which was an output coupler. It was at a distance of approximately 100 mm from the Pr:YLF crystal. The mirror M2 was HR coated for 604 and 302 nm with a radius of curvature of 200 mm, and it was at a distance of approximately 60 mm from M1. The angle of incidence on the M1 mirror in our V-type cavity scheme was approximately 10°. The LBO was placed in the beam waist located close to M2. Calculated based on the ABCD matrix method, the resonator provided a beam waist diameter of approximately 260 μm in Pr:YLF and 140 μm in LBO. The two beam waists both in Pr:YLF and LBO can maximize the efficiency of the second harmonic generation [20].

We obtain a wavelength of 604 nm benefiting from the different polarizations of 604 nm, 607 nm, and 640 nm by adding an uncoated Brewster plate in the resonator. A Brewster plate is a 1-mm-thick glass plate inserted inside the resonator at the Brewster angle. Since the Brewster plate reflects some s-polarized light, but no p-polarized light, the round-trip loss for the s-polarized light is higher than that of the p-polarized light, and the polarization selection of p-polarized light is provided due to competition between the two modes. When the Brewster plate is placed in the resonator, we can make the incident plane vertical to the polarization of 604 nm. Then, the wavelength of 604 nm can pass through the Brewster plate smoothly as p-polarized light, and 607 nm and 640 nm will be reflected at the Brewster plate as s-polarized light. In this way, the wavelength of 604 nm in the resonator can suppress the high-gain wavelengths of 607 nm and 640 nm.

3. RESULTS AND DISCUSSION

The pump source plays an important role in the design of the laser, which is necessary to laser output. The absorption of the pump source at 444 nm is approximately 760 mW, and at 469 nm, it is approximately 600 mW, using a 8-mm-long Pr:YLF crystal with a low doping concentration of 0.2 at. % Pr^{3+} ions at the maximum output power. The absorption coefficient is 55% at the 444 nm LD of 1.4 W, and 41% at the 469 nm LD of 1.5 W.

In the cavity shown in Fig. 3, the angle of the Brewster plate in the resonator is adjusted to a suitable orientation. At the same time, the laser wavelength is measured using an Ocean Optics spectrometer (HR4000) with the resolution of approximately 0.12 nm. Without the Brewster plate, the fundamental laser wavelength is 607 nm. To carry out the wavelength at 604 nm, we inserted the Brewster plate into the resonator, which was helpful for the π-polarized wavelength at 604 nm to suppress the high-gain wavelength at 607 nm of σ-polarized emission. In our experiment, we measured the fundamental wavelength as shown in Fig. 5.

For the intracavity frequency doubling of 604 nm, a 5-mm-long nonlinear crystal LBO was used. The maximum output power extracted from the resonator was approximately 5 mW with respect to the total pump power of 1.4 W at 444 nm and 1.5 W at 469 nm. The central wavelength of the UV laser was 302 nm with a spectral linewidth of 0.15 nm, as shown in Fig. 6. Finally, a Thorlabs beam profiler (BP209-VIS/M) was used to measure the beam quality and the transverse spatial profile of the laser beam. The values of M^2 in the x and y directions were measured to be 1.17 and 1.13, respectively. The transverse

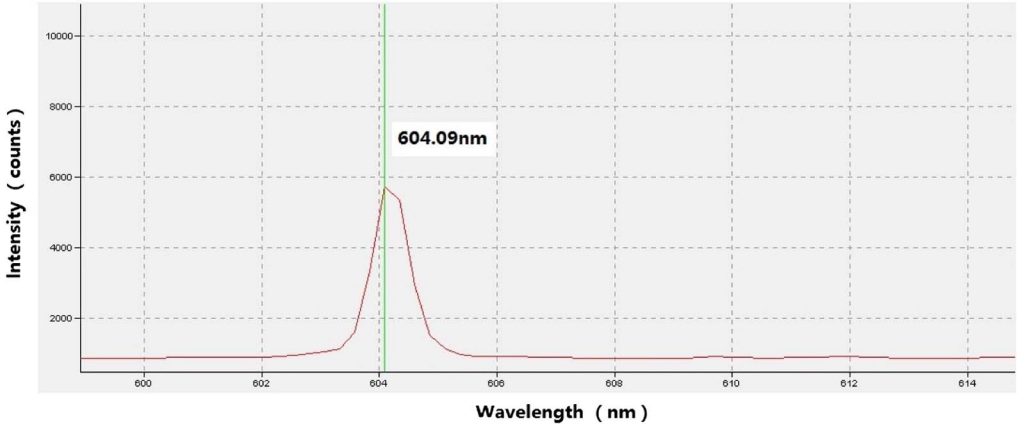

Fig. 5. Spectrum of the UV laser at 604 nm (with the resolution of approximately 0.12 nm).

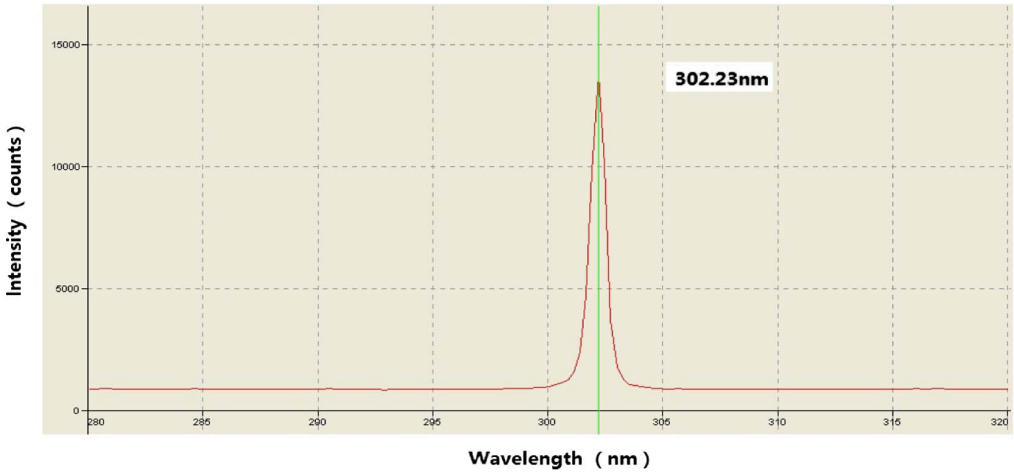

Fig. 6. Spectrum of the UV laser at 302 nm (with the resolution of approximately 0.12 nm).

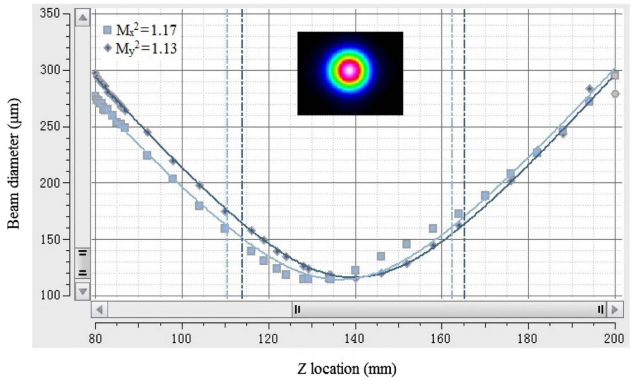

Fig. 7. Beam quality and the transverse spatial profile of the laser beam at 302 nm.

spatial profile of the laser beam was a near-diffraction-limited TEM_{00} mode. Both results are shown in Fig. 7.

A weak UV laser was obtained in our experiment, and we assume that an uncoated LBO used in the resonator and not quite a small beam size in the LBO crystal may have limited the efficiency of our laser system. Further investigation regarding the use of a Brewster-angled LBO, cut for the fundamental laser, and optimization of the resonator design to increase the power of fundamental laser and intensity on the facets of LBO is necessary. The power scaling is still expected if a higher pump power is applied. But we should also take into consideration that the Brewster-angled LBO cut for the fundamental laser may cause loss for second-harmonic wavelength, and an increased intensity on the facets of LBO may reduce the life of laser in further design. Their relationship should be balanced.

4. CONCLUSION

In conclusion, we have demonstrated a compact all-solid-state UV laser operation at 302 nm using a 5-mm-long LBO crystal intracavity frequency doubling of a Pr:YLF laser, pumped by a combined 1.4 W blue LD at 444 nm and 1.5 W blue LD at 469 nm. A 1-mm-thick glass plate was inserted inside the resonator at the Brewster angle in order to in favor the 604 nm lasing. We obtained the maximum output power of approximately 5 mW with respect to the total pump power from a 0.2 at. % Pr:YLF with an 8 mm thickness. The appearance of the Pr:YLF-based laser at 302 nm will also promote the development of the SO_2 gas trace detection technology, in particular, a highly sensitive SO_2 photoacoustic sensor for the application of the SF_6 decomposition detection in electric power systems.

Funding. Changchun Science and Technology Project of China (16SS18).

REFERENCES

1. N. Aubert, T. Georges, C. Chauzat, R. L. Bras, and P. Féron, "Diode-pumped low noise CW 355 nm intra-cavity tripled laser up to 20 mW," Proc. SPIE **6190**, 61900E (2006).
2. Z. Liu, Z. Cai, S. Huang, C. Zeng, Z. Meng, Y. Bu, Z. Luo, B. Xu, H. Xu, C. Ye, F. Stareki, P. Camy, and R. Moncorgé, "Diode-pumped Pr^{3+}:$LiYF_4$ continuous-wave deep red laser at 698 nm," J. Opt. Soc. Am. B **30**, 302–305 (2013).
3. A. Richter, E. Heumann, E. Osiac, G. Huber, W. Seelert, and A. Diening, "Diode pumping of a continuous-wave Pr^{3+}-doped $LiYF_4$ laser," Opt. Lett. **29**, 2638–2640 (2004).
4. A. Richter, E. Heumann, G. Huber, V. Ostroumov, and W. Seelert, "Power scaling of semiconductor laser pumped praseodymimum lasers," Opt. Express **15**, 5172–5178 (2007).
5. T. Gün, P. Metz, and G. Huber, "Power scaling of laser diode pumped Pr^{3+}:$LiYF_4$ CW lasers efficient laser operation at 522.6, 545.9, 607.2, and 639.5 nm," Opt. Lett. **36**, 1002–1004 (2011).
6. B. Xu, P. Camy, J. L. Doualan, Z. Cai, and R. Moncorgé, "Visible laser operation of Pr^{3+}-doped fluoride crystals pumped by a 469 nm blue laser," Opt. Express **19**, 1191–1197 (2011).
7. S. Huang, Z. Liu, C. Zeng, Z. Cai, and H. Xu, "Blue laser diode pumped Pr: YLF green laser," Chin. J. Lasers **39**, 1202005 (2012).
8. V. Ostroumov, W. Seelert, L. Hunziker, and C. Ihli, "522/261 nm CW generation of Pr:YLF laser pumped by OPS laser," Proc. SPIE **6451**, 645104 (2007).
9. V. Ostroumov and W. Seelert, "1 W of 261 nm CW generation in a Pr^{3+}:$LiYF_4$ laser pumped by an optically pumped semiconductor laser at 479 nm," Proc. SPIE **6871**, 68711K (2008).
10. P. Zhu, C. Zhang, K. Zhu, Y. Ping, P. Song, X. Sun, F. Wang, and Y. Yao, "303 nm continuous wave ultraviolet laser generated by

intracavity frequency-doubling of diode-pumped Pr^{3+}:$LiYF_4$ laser," Opt. Laser Technol. **100**, 75–78 (2018).
11. A. Richter, N. Pavel, E. Heumann, G. Huber, D. Paris, A. Toncelli, M. Tonelli, A. Diening, and W. Seelert, "Continuous-wave ultraviolet generation at 320 nm by intracavity frequency doubling of red-emitting praseodymium lasers," Opt. Express **14**, 3282–3287 (2006).
12. Z. Liu, Z. P. Cai, B. Xu, C. Zeng, S. Huang, F. Wang, Y. Yan, and H. Xu, "Continuous-wave ultraviolet generation at 349 nm by intracavity frequency doubling of a diode-pumped Pr:$LiYF_4$ laser," IEEE Photon. J. **5**, 1500905 (2013).
13. V. Ostroumov, W. Seelert, L. Hunziker, A. Richter, and G. Huber, "UV generation by intracavity frequency doubling of an OPS-pumped Pr:YLF laser with 500 mW of CW power at 360 nm," Proc. SPIE **6451**, 645103 (2007).
14. G. Somesfalean, Z. G. Zhang, M. Sjöholm, and S. Svanberg, "All-diode-laser ultraviolet absorption spectroscopy for sulfur dioxide detection," Appl. Phys. B **80**, 1021–1025 (2005).
15. X. Yin, L. Dong, H. Wu, H. Zheng, W. Ma, L. Zhang, W. Yin, L. Xiao, S. Jia, and F. K. Tittel, "Highly sensitive SO_2 photoacoustic sensor for SF6 decomposition detection using a compact mW-level diode-pumped solid-state laser emitting at 303 nm," Opt. Express **25**, 32581 (2017).
16. G. Huber, A. Richter, and E. Heumann, "Continuous wave Praseodymium solid state lasers," Proc. SPIE **6451**, 645102 (2007).
17. L. Esterowitz, F. J. Bartoli, R. E. Allen, D. E. Wortman, C. A. Morrison, and R. P. Leavitt, "Energy levels and line intensities of Pr^{3+} in $LiYF_4$," Phys. Rev. B **19**, 6442–6455 (1979).
18. J. L. Adam, W. A. Sibley, and D. R. Gabbe, "Optical absorption and emission of $LiYF_4$:Pr^{3+}," J. Lumin. **33**, 391–407 (1985).
19. Y. Cheng, B. Xu, B. Qu, S. Luo, H. Yang, H. Xu, and Z. Cai, "Comparative study on diode-pumped continuous wave laser at 607 nm using differently doped Pr^{3+}:$LiYF_4$ crystals and wavelength tuning to 604 nm," Appl. Opt. **53**, 7898–7902 (2014).
20. D. Kleinman, A. Ashkin, and G. Boyd, "The second-harmonic generation of light by focused laser beams," IEEE J. Quantum Electron. **2**, 119 (2003).